Enhanced Performance of Printed Organic Diodes Using a Thin Interfacial Barrier Layer

Kaisa E. Lilja,*,† Himadri S. Majumdar,‡ Fredrik S. Pettersson,‡ Ronald Österbacka,‡ and Timo Joutsenoja†

Department of Electronics, Tampere University of Technology, P.O. Box 692, FI-33101 Tampere, Finland, and Department of Physics, Åbo Akademi University, Porthansgatan 3, FI-20500, Turku, Finland

ABSTRACT Printed, organic diodes with a thin organic interfacial layer forming a Schottky barrier were fabricated and characterized. Experiments indicated that the thickness of the barrier layer is <10 nm. The interfacial layer reduces the reverse current of the diode by 2 orders of magnitude without significantly affecting the forward characteristics above 1 V. As a result, printed organic diodes with a rectification ratio of 5 orders of magnitude were fabricated. The diodes enable applications where low reverse currents are needed.

KEYWORDS: interfacial barrier • organic diode • gravure printing

INTRODUCTION

The development of organic electronic components offers the possibility to manufacture flexible and lightweight electronics using cost-effective processes. Diodes, for example, are generally used as switches, where fast switching between forward and reverse bias is important. Naturally, a very low reverse current is also needed. Certain applications, such as organic diode rectifiers and diode display driving circuits, require sufficient rectification ratios and therefore low reverse currents (1−3). To reach high rectification ratios, a high Schottky barrier is needed. For the cathode, low-work-function metals such as aluminum are preferable but they suffer from oxidation, which results in a voltage offset in the diode forward characteristics (4). Copper does not suffer from oxidation to the same extent as aluminum but has a higher work function and therefore diodes with copper cathodes should exhibit a lower rectification ratio. However, we have previously reported organic printed diodes with copper cathodes and rectification ratios as high as four to 5 orders of magnitude (1). In this work, we show that this result is due to a thin organic interfacial layer on the copper cathode, which prevents hole injection into the organic semiconductor in reverse bias without affecting the forward bias current.

In inorganic metal−insulator-semiconductor (MIS) devices where the insulating SiO_2 thickness is below 7 nm, the charge carriers tunnel through the insulating barrier (5). In MIS Schottky diodes, this causes a reduction in the reverse saturation current and an increase in the barrier height (6). In organic light emitting diodes and electroluminescent devices, a thin interfacial LiF -layer is generally used to enhance electron injection, where a reduction of the barrier height by an alteration in the energy band line-up and charge carrier tunneling has been observed (7, 8). Also polymeric thin insulating films have been used to enhance the efficiency (9). For Schottky diodes, organic interfacial layers have been reported for inorganic and organic semiconductors (10, 11). However, in these reports, the insulating layer is 50−200 nm thick and thus charge carriers cannot cross the barrier by tunneling. Furthermore, such a thick a layer will introduce an extra capacitance at the interface. Here, we report a 5−10 nm thick organic interfacial layer in a printed organic diode. Because of the thin interfacial layer, the reverse current of the diode is significantly reduced without affecting the forward characteristics above 1 V.

EXPERIMENTAL SECTION

The diodes were fabricated on metallized polyester (poly(ethylene terephthalate), PET) film, Melinex ST506 from Dupont Teijin Films, using roll-to-roll compatible printing processes. A copper, silver, or platinum cathode layer was either vacuum evaporated or sputtered onto the PET film and patterned by shadow masking or wet etching. The semiconductor layer, polytriarylamine (PTAA), was printed with a laboratory-scale gravure printing press, Labratester Automatic from Norbert Schläfli Maschinen, and cured at 115 °C for 5 min. The anode material, silver ink PM460A from Acheson Industries Ltd., was also deposited with the gravure press and cured at 115 °C for 5 min. Before fabricating the diodes, the patterned metal substrates were cleaned by rinsing with deionized water and 2-propanol. The diodes were fabricated in a dust-free environment (noncertified but close to ISO 14644−1 class 5) at room temperature and relative humidity of 40−50%.

The DC $J-V$ characteristics of the diodes were measured using a Keithley 236 source-measure unit. Ten samples per each diode structure were measured. The work-function measurements were done with a Kelvin probe setup that has been calibrated and optimized using a sputtered gold electrode (4.6 eV). The relatively low work function of the reference gold can be attributed to contamination on the gold surface (12). The diode thickness was estimated from capacitance measurements that were done with HP 8752A Network Analyzer. Using the

* Corresponding author. E-mail: kaisa.lilja@tut.fi.
Received for review October 12, 2010 and accepted December 1, 2010
† Tampere University of Technology.
‡ Åbo Akademi University.
DOI: 10.1021/am1009869

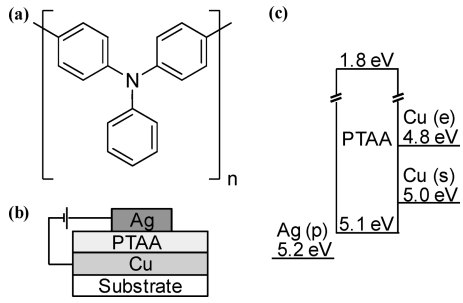

FIGURE 1. (a) Molecular structure of PTAA, (b) structure of printed diodes, (c) schematical energy band diagram for printed silver [Ag (p)], PTAA, evaporated copper [Cu (e)], and sputtered copper [Cu (s)].

relative permittivity of the semiconductor ($\varepsilon_r = 3$, ref 13.) and the active area 4 mm^2, the measured capacitance value of 71 pF translates into a thickness of 1.5 μm. XPS (X-ray photoelectron spectroscopy) was used to determine the elementary structure of the two copper surfaces. All measurements were made in ambient laboratory conditions.

RESULTS AND DISCUSSION

In the printed structure, the silver acts as the anode and the copper as the cathode. Figure 1a presents the molecular structure of PTAA and Figure 1b shows the cross-sectional diode structure. Figure 1c presents a schematical energy band diagram of the diode. The HOMO (highest occupied molecular orbital) and LUMO (lowest unoccupied molecular orbital) levels for PTAA lie at 5.1 and 1.8 eV, respectively (14). The ohmic contact is formed between the printed silver and the HOMO of PTAA, where the measured high work function of the printed silver (5.2 V) indicates the presence of silver oxide on the surface (15, 16), which is likely due to the processing of the silver ink in air. The measured work functions of the evaporated and sputtered copper were 4.8 and 5.0 eV, forming Schottky energy barriers of 0.3 and 0.1 eV, respectively. To confirm that the printed silver contact acts as the anode, we fabricated diodes with platinum and silver contacts. Platinum and silver both had work functions of 5.0 eV.

The $J-V$ characteristics for diodes with four different cathode metals are presented in Figure 2. In forward bias, all diodes have similar behavior and the current density at 5 V is 2 − 3 mA/cm^2. Diodes with silver and platinum cathodes have close to symmetrical $J-V$ characteristics as expected based on the work function measurements. However, the diodes with different copper cathodes differ significantly in their reverse performance; at −5 V, the diodes with evaporated copper cathodes had a current density of 2.5 μA/cm^2 and the diodes with sputtered copper cathodes 20 nA/cm^2. Because the Schottky barrier of the diodes with sputtered copper cathodes is the same as with silver and platinum, similar $J-V$ characteristics should also be obtained. However, the reverse current of the diodes with sputtered copper cathodes at −5 V is 5 orders of magnitude lower than that of the diodes with silver and platinum cathodes and 2 orders of magnitude lower than that of the diodes with evaporated copper cathodes. Thus, the rectification ratio is improved from 1×10^3 to 1×10^5 only by changing from one copper substrate to another.

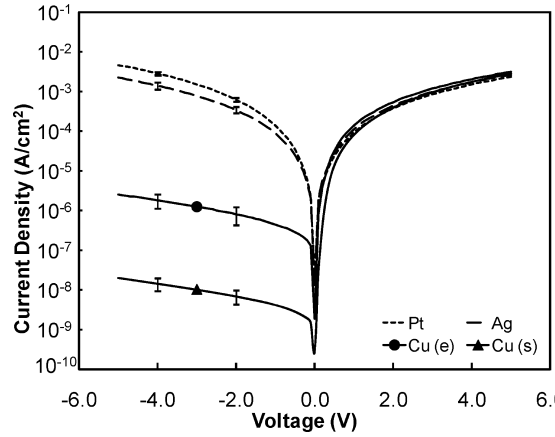

FIGURE 2. $J-V$ performance of diodes with different cathodes. The error bars at −2 and −4 V represent the standard deviation of 10 measured samples.

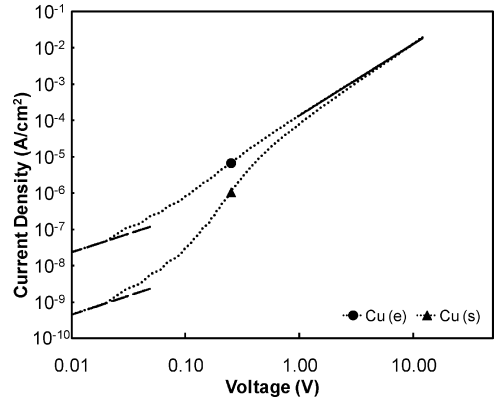

FIGURE 3. Log J−log V characteristics for diodes with evaporated and sputtered copper cathodes. The dashed line represents a slope of 1. The solid line represents a power law with a slope of two from 1 to 12 V. The $J-V$ characteristics were measured up to 12 V.

In general, the current in an organic semiconductor can either be contact or bulk (space-charge) limited. If the current is bulk limited, it obeys eq 1, known as Child's law (13, 17). In eq 1, J is the current density, ε_0 is the permittivity of vacuum, μ is the carrier mobility, V is the applied voltage, and L is the film thickness.

$$J = \frac{9\varepsilon_r\varepsilon_0\mu V^2}{8L^3} \quad (1)$$

The double-logarithmic $J-V$ characteristics for diodes with sputtered and evaporated copper cathodes are shown in Figure 3. For evaporated copper the current is initially ohmic and turns to space-charge limited at around an applied voltage of 0.2 V. Using $\varepsilon_r = 3$ and the measured semiconductor thickness of 1.5 μm, a semiconductor mobility of 1.4 $\times$ 10^{-3} cm^2/(V s) was obtained from eq 1, which is close to the value 2 $\times$ 10^{-3} cm^2/(V s) reported in previous PTAA work (18). For sputtered copper the current is injection limited up to about 2 V, above which the current approaches space-charge limited behavior. Thus, interfacial effects play a role up to at least 2 V in the diodes that have sputtered copper cathodes.

According to the work function measurements, the diodes with evaporated copper cathodes have a Schottky barrier that is 0.2 eV higher than that of the diodes with sputtered copper cathodes and should thus exhibit a higher rectification ratio. However, the $J-V$ characteristics contradict this by showing that the rectification ratio is higher with sputtered copper. Therefore, the difference in the diode $J-V$ characteristics with these two diodes is likely due to the copper−semiconductor interface. Because copper cathodes were used for both diodes, the difference in the diode characteristics arises from the elementary structure of the copper surface. XPS was used to determine the elementary composition of the two copper surfaces. The evaporated copper surface had a structure where elementary copper is clearly visible but oxygen is also detected. In contrast, the sputtered copper surface had only little elementary copper and distinct peaks of oxygen and carbon, indicating that the surface is covered with an organic layer. When both copper surfaces were sputtered with argon (5 nm sputtering depth in the case of SiO_2), the elementary structures on the surfaces became similar. The sputtered copper surface is initially formed in a vacuum chamber, where organic matter from the substrate is amply available. The XPS results strongly suggest that a thin organic layer is formed onto the copper surface during the sputtering process. A layer thickness of 5−10 nm or less was estimated on the basis of the argon sputtering. Bond breaking and redeposition of polystyrene after ion bombardment has been studied previously by Netcheva and Bertrand (19). They note that polystyrene can be redeposited on the surface during Ar^+ ion sputtering depending on the process parameters. Furthermore, they note a great number of hydrocarbon fragments on the polystyrene film after the process. They attributed this to be a signature of hydrocarbon coming from external atmosphere that is adsorbed at strongly reactive radical sites created by ion irradiation. Our results indicate that a close to similar process takes place on the surface of the sputtered copper.

It can be argued that the thin organic interfacial layer on the sputtered copper substrate acts as an extra barrier at the Schottky interface. Previously, the effect of a thin PMMA layer between the cathode electrode and the semiconductor has been discussed for polymer electroluminescence devices (9). It was speculated that the injected charge carriers accumulate at the interface between the semiconductor and the insulator. This model can now be further expanded on the basis of our results and is illustrated in Figure 4 where charge carrier movement and energy band diagrams are presented under open circuit, forward bias, and reverse bias for diodes without (top) and with (bottom) the organic interfacial layer. Under open circuit (Figure 4a,d), there is no net movement of charge carriers. Under forward bias (above 0.2 V), the charge carriers move easily from the anode to the cathode in diodes without the organic interfacial layer (Figure 4b) and the current is close to space-charge limited. However, in the diodes with the organic interfacial layer (Figure 4e) at low voltages, the charge carriers accumulate at the interfacial layer and the diode is injection limited. As the bias increases, charge carriers tunnel through the interfacial barrier and the current approaches space-charge limited behavior. In reverse bias, noticeable reverse current can be observed in the diodes without the organic interfacial layer (Figure 4c). In contrast, in the diodes with the interfacial layer (Figure 4f) the charge carriers have to cross a tunneling barrier of ∼5−10 nm in addition to the energy barrier of 0.1 eV. In this case, there is no accumulated space charge that could create a sufficient field across the barrier to assist the tunneling process, which results in a very low reverse current. As a result, the interfacial layer lowers the reverse current of the diodes by 2 orders of magnitude and significantly improves the diode rectification ratio.

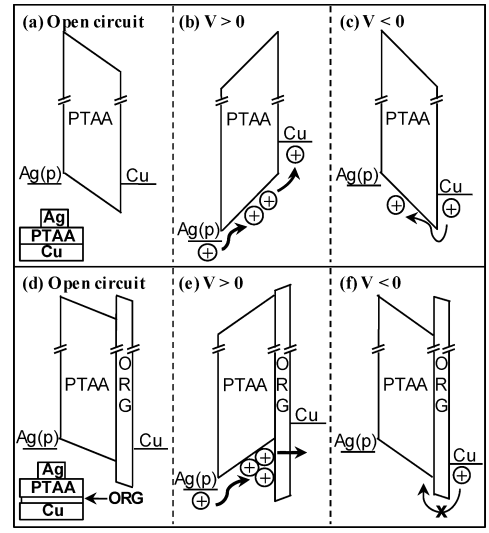

FIGURE 4. Schematical energy band diagram for diodes under open circuit, forward bias and reverse bias conditions. Illustrations of (a−c) diodes without the interfacial layer and (d−f) diodes with the interfacial layer. The arrows represent charge carrier (hole) movement.

Because the interfacial layer prevents charge carrier injection from copper to PTAA, generally all insulating layers with similar thicknesses have the same effect and can therefore be used to maximize the rectification ratio of the printed diodes. Optimally, the layer is formed using a cost-effective process such as coating or printing but generally the layer thicknesses produced by these methods are in the order of micrometers or more. Initial experiments indicate that a 5 nm evaporated lithium fluoride (LiF) layer (evaporated at a pressure of 2×10^{-5} mbar) on top of evaporated copper and silver cathodes reduces the reverse current of the diode by 2 orders of magnitude resulting in the same effect as described in figure 4. If an evaporated interfacial layer such as LiF withstands the wet etching patterning process, it can be used as a part of a cost-effective manufacturing process to fabricate diodes with a high rectification ratio.

CONCLUSIONS

In conclusion, organic Schottky diodes with different electrodes were fabricated. A 5−10 nm thick insulating interfacial layer was observed at the Schottky interface, which increases the barrier and reduces the diode reverse

current by 2 orders of magnitude. However, because the charge carriers can tunnel through the barrier, the forward characteristics above 1 V remain unchanged. This study thus shows the possibility of using thin organic interfacial layers in printed organic Schottky diodes for applications that require high rectification ratios and low reverse currents.

Acknowledgment. The authors acknowledge UPM-Kymmene Corporation for financial support and Merck Chemicals Ltd. for providing the semiconductor material. Åbo Akademi University also acknowledges partial financial support from the Academy of Finland through the Center of Excellence program.

REFERENCES AND NOTES

(1) Lilja, K. E.; Bäcklund, T. G.; Lupo, D.; Hassinen, T.; Joutsenoja, T. *Org. Electron.* **2009**, *10*, 1011–1014.
(2) Steudel, S.; Myny, K.; Arkhipov, V.; Deibel, C.; de Vusser, S.; Genoe, J.; Heremans, P. *Nat. Mater.* **2005**, *4*, 597–600.
(3) Lilja, K. E.; Bäcklund, T. G.; Lupo, D.; Virtanen, J.; Hämäläinen, E.; Joutsenoja, T. *Thin Solid Films.* **2010**, *518*, 4385–4389.
(4) Raja, M.; Sedghi, N.; Badriya, S.; Higgins, S. J.; Lloyd, G. C. R.; Eccleston, W. *Proceedings of ESSDERC 2005*; IEEE: Piscataway, NJ, 2005; 3.B.2.
(5) Sze, S. M.; Ng, K. K. *Physics of Semiconductor Devices*, 3rd ed.; John Wiley & Sons: New York, 2007; pp 417–437.
(6) Hudait, M. K.; Krupanidhi, S. B. *Solid-State Electron.* **2000**, *44*, 1089–1097.
(7) Brown, T. M.; Millard, I. S.; Lacey, D. J.; Burroughes, J. H.; Friend, R. H.; Cacialli, F. *Synth. Met.* **2001**, *124*, 15–17.
(8) Hung, L. S.; Tang, C. W.; Mason, M. G. *Appl. Phys. Lett.* **1997**, *70*, 152–154.
(9) Kim, Y.-E.; Park, H.; Kim, J.-J. *Appl. Phys. Lett.* **1996**, *69*, 599–601.
(10) Güllü, Ö.; Türüt, A. *J. Appl. Phys.* **2009**, *106*, 103717.
(11) Kuo, C. S.; Wakim, F. G.; Sengupta, S. K.; Tripathy, S. K. *J. Appl. Phys.* **1993**, *74*, 2957–2958.
(12) Wan, A.; Hwang, J.; Amy, F.; Kahn, A. *Org. Electron.* **2005**, *6*, 47–54.
(13) Jain, S. C.; Willander, M.; Kumar, V. *Conducting Organic Materials and Devices*; Elsevier: New York, 2007; pp 27−31.
(14) Schols, S.; Verlaak, S.; Rolin, C.; Cheyns, D.; Genoe, J.; Heremans, P. *Adv. Funct. Mater.* **2008**, *18*, 136–144.
(15) Narioka, S.; Ishii, H.; Yoshimura, D.; Sei, M.; Ouchi, Y.; Seki, K.; Hasegawa, S.; Miyazaki, T.; Harima, Y.; Yamashita, K. *Appl. Phys. Lett.* **1995**, *67*, 1899–1901.
(16) Barik, U. K.; Srinivasan, S.; Nagendra, C. L.; Subrahmanyam, A. *Thin Solid Films* **2003**, *429*, 129–134.
(17) Campbell, A. J.; Bradley, D. D. C.; Lidzey, D. G. *J. Appl. Phys.* **1997**, *82*, 6326–6342.
(18) Veres, J.; Ogier, S.; Leeming, S.; Brown, B.; Cupertino, D. *Mater. Res. Soc. Symp. Proc.* **2002**, *708*, BB8.7.1.
(19) Netcheva, S.; Bertrand, P. *Polym. Sci., Part B: Polym. Phys.* **2001**, *39*, 314–325.

AM1009869